Journal of Hazardous Materials 170 (2009) 633–638

Contents lists available at ScienceDirect

Journal of Hazardous Materials

journal homepage: www.elsevier.com/locate/jhazmat

Abatement of toluene from gas streams via ferro-electric packed bed dielectric barrier discharge plasma

Wenjun Liang*, Jian Li, Jie Li, Yuquan Jin

College of Environmental & Energy Engineering, Beijing University of Technology, No. 100 Ping Le Yuan, Chao Yang District, Beijing 100124, PR China

ARTICLE INFO

Article history:
Received 14 February 2009
Received in revised form 4 May 2009
Accepted 5 May 2009
Available online 18 May 2009

Keywords:
Dielectric barrier discharge plasma
Ferro-electric packed bed
Toluene
Ozone
Specific energy density
Energy yield

ABSTRACT

Destruction of gaseous toluene via ferro-electric packed bed dielectric barrier discharge plasma in a coaxial cylindrical reactor was carried out at atmospheric pressure and room temperature. The difference among three kinds of reactors was compared in terms of specific energy density (SED), energy yield (EY), toluene decomposition. In order to optimize the geometry of the reactor, the removal efficiency of toluene was compared for various inner electrode diameters. In addition, qualitative analysis on by-products and particular discussion on toluene abatement mechanisms were also presented. It has been found that ferro-electric packed bed DBD reactor could effectively decompose toluene. Toluene removal efficiency enhanced with increasing SED. With respect to toluene conversion, 1.62 mm electrode appeared to be superior to 1.06 mm electrodes. $BaTiO_3$ reactor had the highest toluene removal efficiency among the reactors. For $NaNO_2$ reactor, the highest EY could reach 17.0 mg/kWh to a certain extent.

1. Introduction

Besides sulphur and nitrogen oxides, volatile organic compounds (VOCs) are considered to be primary toxic air pollutants in industrial and urban areas. Toluene is one of them and is harmful to human body especially to nerve system. The conventional means for VOCs abatement include adsorption, condensation, incineration, and catalytic oxidation. But these means have been restricted for their drawbacks, such as adsorbent could be invalid because of some aerosol particles, while condensation, incineration and catalytic oxidation need high cost and energy consumption. In recent years, non-thermal plasma (NTP) has great industrial potential for the moderate operation conditions (normal temperature and atmospheric pressure), moderate capital cost, compact system, easy operations and short residence times. Nowadays, NTP technology has been applied to the decomposition of VOCs [1–6]. Furthermore, ferro-electric packed bed dielectric barrier discharge (DBD) plasma reactor has been widely investigated for application to the VOCs treatment because this type of reactor can generate extremely high-energy electrons [7–11]. In this type of reactor, the electrical energy fed into the discharges is used preferentially to create energetic electrons instead of heating the ions and the neutral gas molecules. The energetic electrons are employed directly to dissociate and ionize the pollutants as well as carrier gas molecules to produce various radicals to react with and convert a part of pollutants [12]. $BaTiO_3$ was used as ferro-electrics with displacive type in all the literature published. Moreover, in most studies, pollutants were removed under static state or low flow case (gas flow rate = 0.1–1 l/min), which was lower than gas rate of factual industrial exhausts. There have little reports on VOCs treatment under high flow rate.

In the present paper, we developed a new ferro-electric packed bed dielectric barrier discharge plasma reactor, in which $NaNO_2$ was used as one of the typical ferro-electrics with order–disorder type. The difference among three kinds of reactors ($BaTiO_3$ ferro-electric reactor, $NaNO_2$ ferro-electric reactor and none ferro-electric reactor) was compared in terms of specific energy density (SED), energy yield (EY), toluene decomposition. Toluene abatement in $NaNO_2$ reactor was also systematically investigated. Finally, by-products and mechanism of toluene abatement were analyzed. The aim of this paper is to provide full-scale analysis to toluene destruction, which will give some advisable proposals to commercial availability.

2. Experimental details

2.1. Experimental setup

The schematic diagram of the experimental setup for the present study was shown in Fig. 1, which consisted of a ferro-electric packed bed reactor, an high-frequency AC power supply (0–20 kV, 0–50 kHz, sine wave), a continuous flow gas supplying system as

* Corresponding author.
E-mail address: liangwenj1978@hotmail.com (W. Liang).

0304-3894/$ – see front matter © 2009 Elsevier B.V. All rights reserved.
doi:10.1016/j.jhazmat.2009.05.019

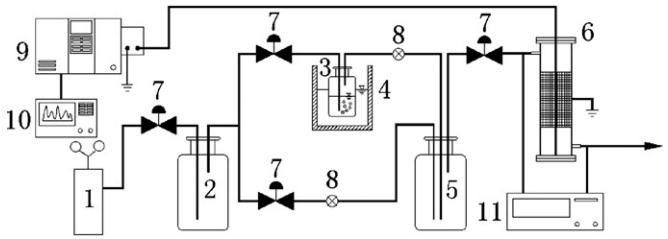

Fig. 1. Schematic diagram of the experimental setup. (1) Compressed air cylinder; (2) buffer; (3) toluene liquid bottle; (4) water bath; (5) mixing chamber; (6) ferro-electric packed bed reactor; (7) MFC; (8) needle valve; (9) AC power supply; (10) oscillograph; (11) gas chromatograph.

well as electric and gaseous analytical systems. Toluene was evaporated by bubbling with compressed air. It was then allowed to pass through a mixing chamber for a thorough mixture with air before being introduced into the DBD reactor. The flow rate and toluene concentration were adjusted by mass flow controllers (MFC), which were fixed at 8.5 l/min in the reactor. The coaxial cylindrical DBD reactor was made of quartz glass with an inner diameter of 17.9 mm and wall thickness of 1.2 mm wrapped by the iron mesh of 20 cm length as a ground electrode. The inner discharge electrode was a tungsten wire (1.06, 1.62 mm in diameter, respectively) placed on the axis of the reactor. The relative humidity in the reactor was of 30% controlled with a thermohygrometer.

Ceramic raschig ring was chosen as ferro-electrics carrier because of its shape being of hollow cylinder (9.2 mm o.d., 5.6 mm i.d. and 10.5 mm length) that would attribute to minimize gas flow resistance. $NaNO_2$ (A.R., Yili Chemical Plant, Beijing) or $BaTiO_3$ (Beijing Research Institute of Chemical Engineering and Metallurgy, GWBT) was coated on ceramic raschig ring by means of dip-coating method. After immersion, the coated rings were dried at room temperature and then calcined at 500 °C in muffle for 2 h. After the rings were coated five times, a thin ferro-electrics film (0.5 mm) was coated. The film was very stable and durable without any loss during application. The ferro-electrics raschig rings were packed with the DBD reactor in random.

2.2. Analysis methods

Toluene gas from inlet and outlet were sampled by a gastight syringe, and the concentration were measured by gas chromatography (Agilent 6890N, USA), equipped with a flame ionization detector (FID), and a capillary column of HP-5.

The toluene removal efficiency is calculated by following:

$$\eta_{toluene}\ (\%) = \frac{C_{in} - C_{out}}{C_{in}} \times 100 \quad (1)$$

where C_{in} and C_{out} denote to the inlet and outlet concentration (mg/m^3) of toluene, respectively.

CO and CO_2 in the effluent were analyzed qualitatively by gas chromatography (Agilent 6890N, USA), equipped with a thermal conductivity detector (TCD), and a capillary column of PLOT-Q. Solid depositions on the internal wall and inner discharge electrode of DBD reactor were collected and analyzed by a Fourier transformation infrared spectrometer (FT-IR, Vertex70, Germany). Ozone concentration produced in the reaction was measured by indigo disulfonic acid sodium spectrophotometry.

The specific energy density (SED) was defined as the average power dissipated in the discharge divided by the total gas flow rate, which could be calculated with the following relations:

$$\text{SED}\ (\text{J/l}) = \frac{P\ (\text{W})}{Q\ (\text{l/min})} \times 60 \quad (2)$$

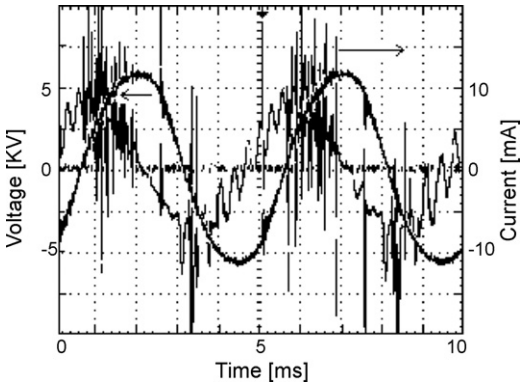

Fig. 2. Typical voltage and current waveforms for DBD (applied voltage: 10 kV).

where P and Q denote to the discharge power (W) and gas flow rate (l/min).

As a measure of the energy efficiency, energy yield (EY) was defined as follows:

$$\text{EY}\ (\text{mg/kWh}) = \frac{C_{in} - C_{out}}{\text{SED}} \quad (3)$$

2.3. Electrical measurements

The voltage and current waves were determined with an oscilloscope (Tektronix 2014, USA). To investigate the electric characteristics of DBD discharge, the voltage applied to the reactor was sampled by a 12,500:1 voltage divider. In order to obtain the total charge and discharge power simultaneously, a capacitor (C_m) was inserted between the reactor and the ground. The electrical power provided to the reactor discharge was measured with Q–V Lissajous diagram representing to be a parallelogram. The discharge power was proportional to the area of parallelogram, which could be calculated according to the relation:

$$P = F \times C_m \times S \quad (4)$$

where C_m was to the measuring capacitance, F was the power frequency and S was the area of parallelogram.

3. Experimental results

3.1. Electrical discharge characteristics

Typical applied voltage and discharge current waveforms for the ferro-electric packed bed reactor tested were shown in Fig. 2. The applied voltages were 10-kVpp (peak-to-peak voltage) sinusoidal waveforms, and were little distorted by the partial discharge current. The discharge voltage and current showed a typical barrier discharge waveforms, that is, the partial discharge current appeared when the applied voltage transited from certain values (discharge onset voltages) to positive or negative maximum. The ferro-electric DBD reactor used in the experiment showed the better discharge characteristics in terms of the discharge current, the electric field strength and the temperature [13].

Fig. 3 showed the variation of SED as a function of applied voltage for the $NaNO_2$ ferro-electric DBD reactor with various electrode diameters: 1.06 and 1.62 mm, respectively. The SED depended almost linearly on the voltage due to the fixed AC frequency (15 kHz). Taken the result of 1.62 mm inner electrode for example, with the increasing of applied voltage from 8 to 13 kV, the SED increased from 230 to 786 J/l. According to the experimental results, it can be found that the bigger size (1.62 mm) electrode was slightly superior to the smaller size (1.06 mm) electrode. The increasing electric field accelerated the electrons, which resulted

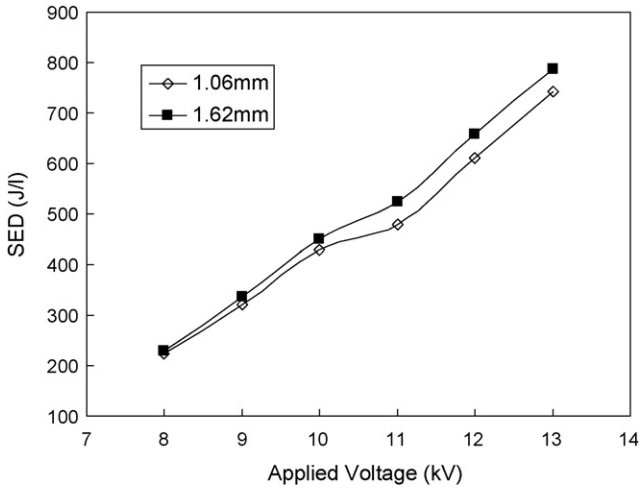

Fig. 3. Variation of SED as a function of applied voltage for $NaNO_2$ DBD reactor.

in producing more micro-discharges and active species in plasma. Moreover, the number of secondary electrons emitted from thick tungsten electrode was more than that from thin electrode, which could stimulate the collision between toluene molecules and electrons.

Fig. 4 showed the variation of SED as a function of applied voltage for various DBD reactors with inner electric diameter of 1.62 mm and fixed AC frequency of 15 kHz. With the increasing of applied voltage, SED of three kinds of reactor increased, the reason of which was that SED was proportional to P and inversely proportional to Q from Eq. (2). Furthermore, the order of SED for the reactors under applied voltage was $BaTiO_3$ reactor > $NaNO_2$ reactor > none ferro-electric reactor. When applied voltage was 13 kV, SED of $BaTiO_3$ reactor, $NaNO_2$ reactor and none ferro-electric reactor was 820, 786 and 690 J/l, respectively. When external AC voltage was applied across the high dielectric layer, $BaTiO_3$ or $NaNO_2$ were polarized, and an intense electric field was formed around each pellet contact point, resulting in partial discharge. As the applied ac voltage increased beyond the corona onset voltage, an increase of plasma activity was visible and the reactor was filled with high-energy free electrons [8], which led to the SED of $BaTiO_3$ or $NaNO_2$ reactor increasing. And because the spontaneous polarization intensity of $BaTiO_3$ (25 $\mu c/cm^2$) was higher than that of $NaNO_2$ (5 $\mu c/cm^2$), $BaTiO_3$ was easily to be polarized, which resulted in the SED of $BaTiO_3$ being higher than $NaNO_2$.

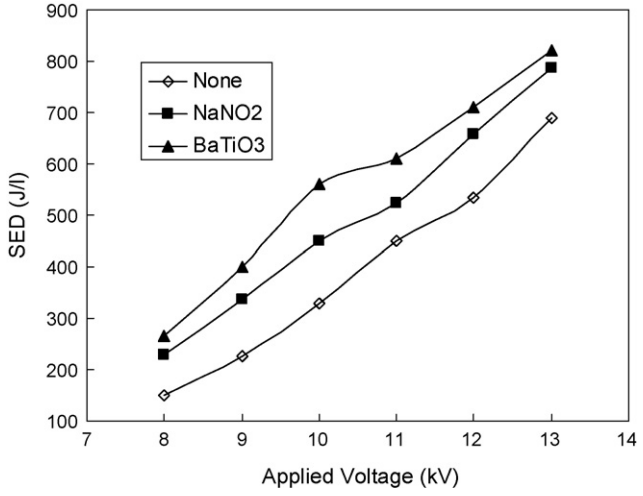

Fig. 4. Variation of SED as a function of applied voltage for different DBD reactors.

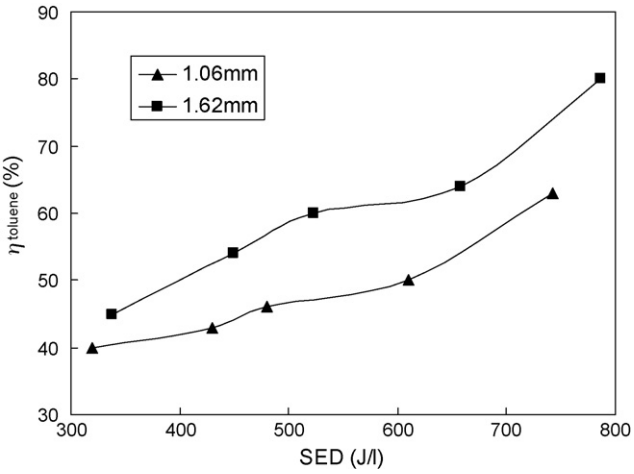

Fig. 5. Toluene abatement as a function of SED for $NaNO_2$ DBD reactor (AC frequency: 15 kHz).

3.2. Toluene abatement in the reactor

Fig. 5 represented the removal process of toluene in $NaNO_2$ DBD reactor as a function of SED for various sizes of wires. The toluene conversion with 1.06 and 1.62 mm inner electrode followed the same trend, that is, $\eta_{toluene}$ enhanced with the increasing of SED. In addition, toluene conversion rate of 1.62 mm electrode with different SED was higher than that of 1.06 mm electrode. For example, toluene abatement efficiency of 1.62 mm electrode reactor increased from 45 to 80% with the increasing of SED in the range of 338–786 J/l, while toluene conversion was of 40–63% with SED of 320–743 J/l for 1.06 mm electrode reactor. With the increasing of SED, energy throughout the entire discharge volume was developing; micro-discharges occurred in the whole reactor in turn and stimulated the chemical reactions between toluene molecules and active electrons. Furthermore, the thick inner electrode has lager superficial area than that of thin electrode, so it has stronger ability to emit more secondary electrons for the reaction.

The effect of ferro-electrics composing DBD reactor on toluene decomposition and SED as a function of AC frequency was plotted in Figs. 6 and 7. According to Eliasson et al. [14], the material of dielectric barrier plays a key role for the proper functioning of the discharge. From the experimental results, it demonstrated that the ferro-electric material employed was an important fac-

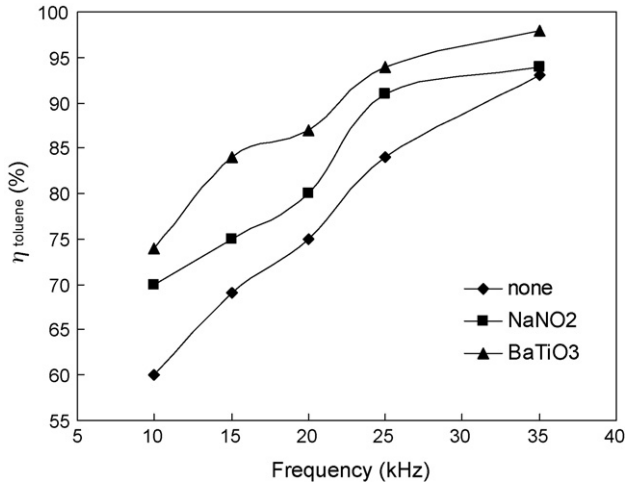

Fig. 6. Toluene abatement as a function of AC frequency for different DBD reactors (inner electrode diameter: 1.62 mm).

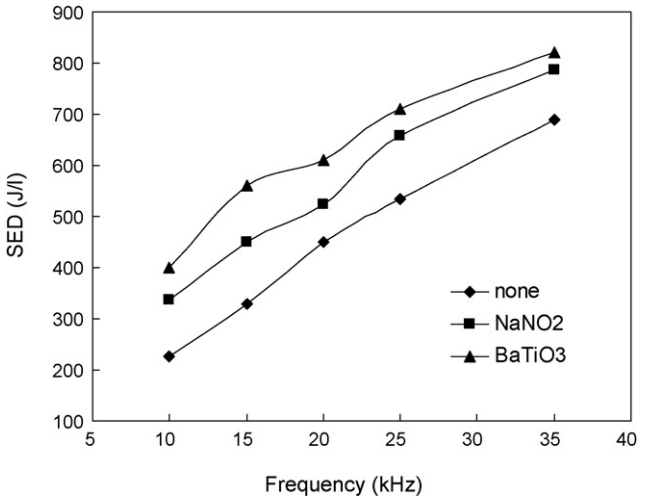

Fig. 7. Variation of SED as a function of AC frequency for different DBD reactors (inner electrode diameter: 1.62 mm).

tor influencing the toluene removal. It was obvious that toluene removal of three reactors was in the order $BaTiO_3$ ferro-electric reactor > $NaNO_2$ ferro-electric reactor > none ferro-electric reactor under the same experimental conditions. Just as illustrated above, in AC electric field, $BaTiO_3$ or $NaNO_2$ could be polarized, which resulted in enhancing the electric field and producing more high-energy electrons contributed to the abatement of toluene. And because the spontaneous polarization intensity of $BaTiO_3$ was larger than that of $NaNO_2$, toluene removal efficiency of $BaTiO_3$ is higher than that of $NaNO_2$. For example, when AC frequency was 25 kHz, toluene removal rates with $BaTiO_3$ ferro-electric reactor, $NaNO_2$ ferro-electric reactor and none ferro-electric reactor were 94, 91 and 84%, respectively. At the same time, SED of three reactors with AC frequency being 25 kHz were 710, 658, and 535 J/l. Just like the relationship between SED and applied voltage, SED increased with the enhancement of AC frequency in all reactors.

3.3. Energy efficiency for toluene removal

In order to discuss the toluene removal ability of the plasma reactor, energy yield was used. From the Eq. (3), it can be seen that EY is in inverse ratio with SED. Fig. 8 illustrated the relationship between EY and SED for $NaNO_2$ DBD reactor when the AC frequency was 15 kHz. Obviously, EY decreased with the increasing of SED for $NaNO_2$ DBD reactor. As SED ascended from 230 to 786 J/l, EY descended from 17.0 to 4.97 mg/kWh. Fig. 9 showed the toluene abatement efficiency and energy filed as functions of AC

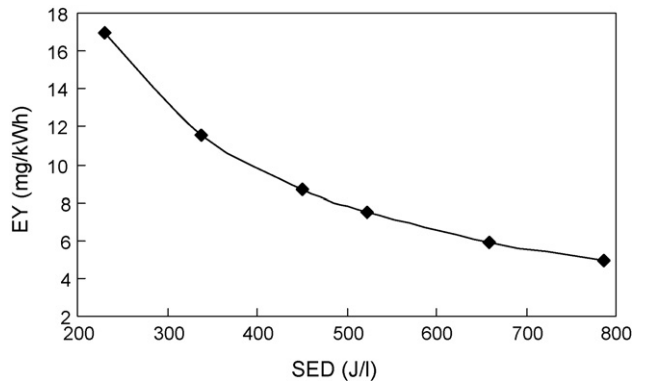

Fig. 8. Energy yield as a function of SED for $NaNO_2$ DBD reactor (inner electrode diameter: 1.62 mm).

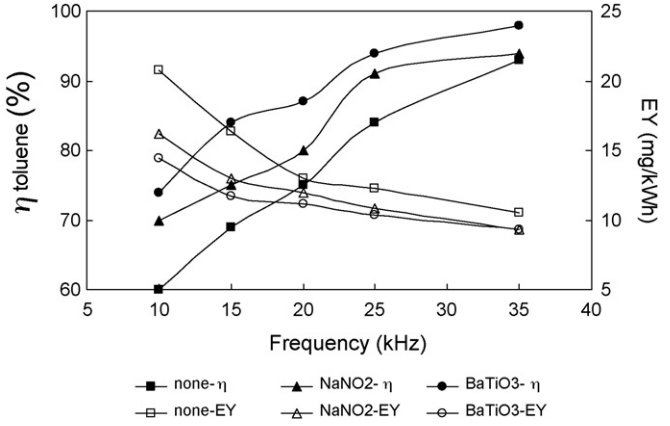

Fig. 9. Toluene abatement and EY as functions of AC frequency for different DBD reactors (inner electrode diameter: 1.62 mm).

frequency for various reactors. At the same AC frequency, with the toluene removal efficiency enhancement, energy field descended for all of reactors. Furthermore, EY of the reactors was in the order $BaTiO_3$ ferro-electric reactor < $NaNO_2$ ferro-electric reactor < none ferro-electric reactor. The highest EY was 20.7 mg/kWh for none ferro-electric reactor when AC frequency was 10 kHz, while the lowest EY was 9.3 mg/kWh for $BaTiO_3$ ferro-electric reactor when AC frequency was 35 kHz. Energy in plasma reactor was used to not only toluene removal, but ferro-electric materials polarization, so EY of $BaTiO_3$ or $NaNO_2$ reactor was lower than none ferro-electric reactor. But the ferro-electric materials polarization could enhance the plasma discharge which increased the toluene removal rate at the same time. So the better matching between energy yield and toluene removal needed to be further considered in future works.

3.4. By-products and mechanism analysis

3.4.1. By-products analysis

One of the most important by-products in a non-thermal plasma discharge was ozone. Oxygen radicals are generated by dissociation of molecular oxygen after impact with accelerated electrons in the corona discharge. Atomic oxygen is a strong oxidizer, but its stability is very limited. Due to fast recombination processes, the lifetime is only a few microseconds at atmospheric pressure [15]. Oxygen radicals are generated by dissociation of molecular oxygen according

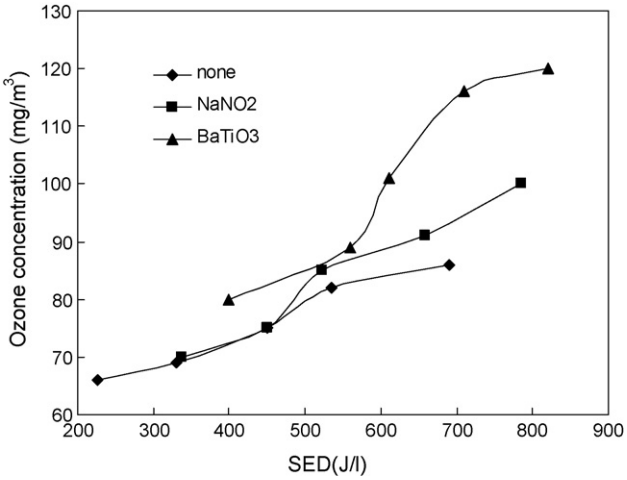

Fig. 10. Ozone outlet concentration as a function of SED (AC frequency: 15 kHz; inner electrode diameter: 1.62 mm).

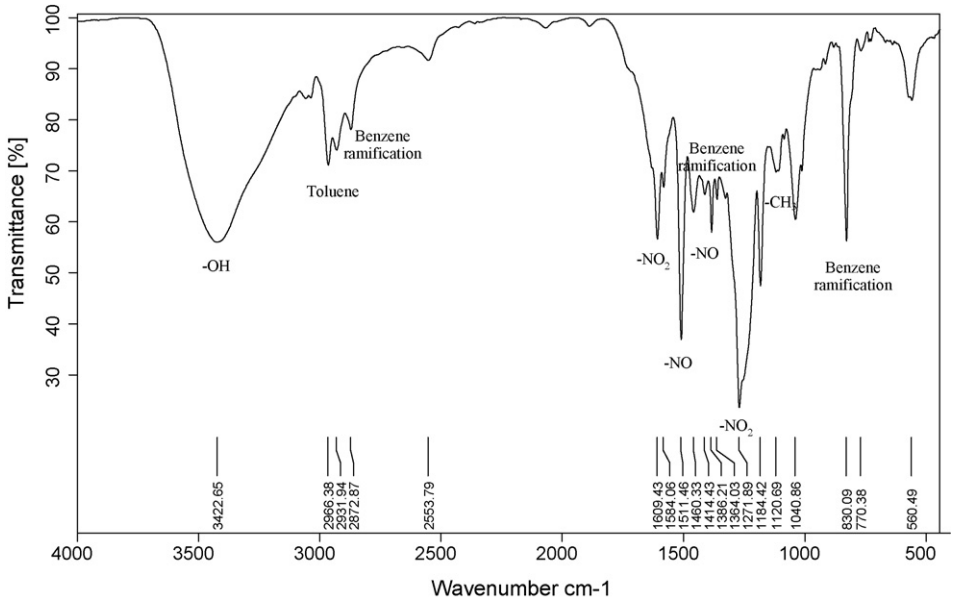

Fig. 11. FT-IR spectrum of solid residues of toluene destruction in $NaNO_2$ DBD.

to the reaction:

$$e + O_2 \rightarrow e + O + O$$

Atomic oxygen reacts with molecular oxygen in three-body collisions, forming ozone by the following reaction:

$$O + O_2 + M \rightarrow O_3 + M$$

In air, M can be either molecular oxygen or molecular nitrogen [16]. Ozone is a more stable molecule; its lifetime at room temperature is several days. Ferro-electric materials affect the ozone production; Fig. 10 showed an increase of ozone outlet production with increasing SED of three reactors. From mentioned above, due to the polarization and spontaneous polarization intensity of $BaTiO_3$ or $NaNO_2$, we can concluded that the amounts of high-energy electrons and atomic oxygen in different reactors was in the order $BaTiO_3$ ferro-electric reactor > $NaNO_2$ ferro-electric reactor > none ferro-electric reactor. So ozone outlet concentration of the reactors was in the order $BaTiO_3$ ferro-electric reactor > $NaNO_2$ ferro-electric reactor > none ferro-electric reactor. The highest concentration for an energy density of 820 J/l was 120 mg/m^3 for $BaTiO_3$ ferro-electric reactor, while the lowest concentration decreased to 66 mg/m^3 for none ferro-electric reactor.

Only CO, CO_2 and H_2O were detected from the outlet effluent; no other products of partial oxidation were found by on-line GC analysis. Analyzing outlet gas by FT-IR, no new strong bands were found. But it was unsure that toluene was decomposed totally on basis of these phenomena because perhaps the content of some by-products were less than the measurement limit of GC or FT-IR. In addition, in the inner wall of DBD tube and the ferro-electric surface, some brown residue occurred, which could dissolve in acetone (C_3H_6O). FT-IR analysis (Fig. 11) had shown that the main possible components of residues taken from toluene plasma were toluene, hydroxyl compound, nitro compound, methyl compound, and benzene ramification. The relative yields of these compounds varied with different conditions.

3.4.2. Reaction mechanism of toluene destruction in DBD

It is well known that toluene molecule is relative stable. Bond energy of C=C in benzene ring is 5.5 eV, while C–C energy between methyl and benzene ring is 3.6 eV, so C–C can easily to be destructed by high-energy electron beyond 3.6 eV. Once benzene ring is ruptured, a series of oxidation reaction will happen subsequently. Possible reactions between electrons and toluene molecules were as follows.

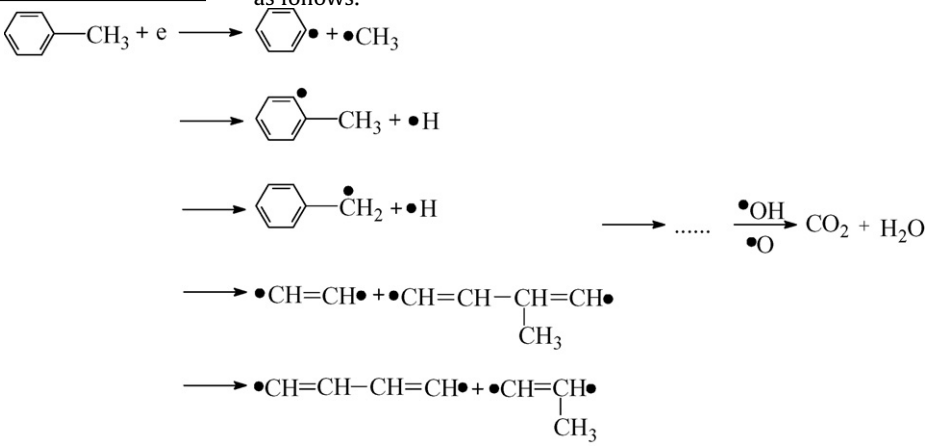

Plasma chemical reaction is a complicated course; pollutant molecules often undergo a series of intermediate reactions before they are completely destructed in plasma. The principle processes of toluene destruction induced by energetic electrons in plasma are electrons and radicals (such as O or O_3).

Firstly, the high-energy electron in plasma attacks oxygen to generate O atom.

$$O_2 \xrightarrow{e} O + O$$

Secondly, O atom behaves as a strong oxidant to produce other oxidation products and radicals such as O_3 or OH.

$$O + O_2 \rightarrow O_3$$

These radical species (O, O_3, OH) react with toluene molecules to form other products or other oxidation products (CO, CO_2, H_2O) by breaking the aromatic structure. These reactions between radical species and toluene molecules were as follows.

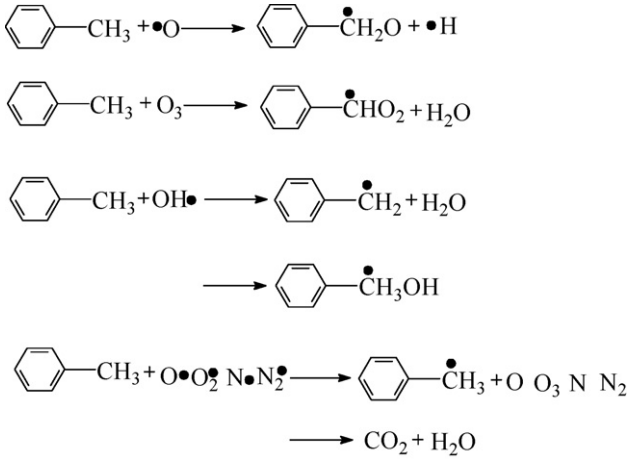

4. Conclusions

The abatement of toluene via ferro-electric packed bed dielectric barrier discharge plasma in a coaxial cylindrical reactor was experimentally investigated. The difference among three kinds of reactors was compared in terms of energy, toluene decomposition. Furthermore, by-products and mechanism of toluene abatement were also analyzed. The main results were summarized as follows.

(1) The SED depended almost linearly on the voltage for $NaNO_2$ ferro-electric DBD reactor. The highest SED could reach 786 J/l as voltage being 13 kV. The bigger size electrode was slightly superior to the smaller size electrode. The order of SED for three reactors was $BaTiO_3$ reactor > $NaNO_2$ reactor > none ferro-electric reactor.

(2) Toluene removal efficiency enhanced with the increasing of SED for all reactors. Attributing to lager superficial area, 1.62 mm electrode appeared to be superior to 1.06 mm electrodes in general with respect to toluene conversion. $BaTiO_3$ reactor had the highest toluene removal efficiency among the reactors. For $NaNO_2$ reactor, EY could reach 17.0 mg/kWh. The highest EY was 20.7 mg/kWh for none ferro-electric reactor.

(3) As an important by-product, ozone concentration increased with higher SED. FT-IR analysis showed many compounds produced in plasma. The reaction mechanisms of toluene in plasma were very complicated due to the attendance of radical species produced in discharge process. Much work needed to be done such as deep investigation of by-products, energy utilizing, and reaction mechanism before industrial application.

Acknowledgements

This work was supported by Youth Scientific Research Fund of BJUT (X1005013200802) and Doctoral Startup Fund of BJUT (52005013200703).

References

[1] C.L. Chang, T.S. Lin, Decomposition of toluene and acetone in packed dielectric barrier discharge reactors, Plasma Chem. Plasma Process. 25 (2005) 227–243.
[2] H.H. Kim, H. Kobara, A. Ogata, S. Futamura, Comparative assessment of different non-thermal plasma reactors on energy efficiency and aerosol formation from the decomposition of gas-phase benzene, IEEE Trans. Ind. Appl. 41 (2005) 206–214.
[3] H. Kohno, A.A. Berezin, J.S. Chang, M. Tamura, T. Yamamoto, A. Shibuya, S. Honda, Destruction of volatile organic compounds used in a semiconductor industry by a capillary tube discharge reactor, IEEE Trans. Ind. Appl. 34 (1998) 953–966.
[4] S.M. Young, M.N. Chang, H.C. Moo, I.S. Nam, Decomposition of volatile organic compounds and nitric oxide by nonthermal plasma discharge processes, IEEE Trans. Plasma Sci. 30 (2002) 408–416.
[5] T. Oda, T. Takahashi, K. Yamaji, TCE decomposition by the nonthermal plasma process concerning ozone effect, IEEE Trans. Ind. Appl. 40 (2004) 1249–1256.
[6] Z.L. Ye, Y.N. Zhang, P. Li, L.Y. Yang, R.X. Zhang, H.Q. Hou, Feasibility of destruction of gaseous benzene with dielectric barrier discharge, J. Hazard. Mater. 156 (2008) 356–364.
[7] H.L. Chen, H.M. Lee, S.H. Chen, M.B. Chang, Review of packed-bed plasma reactor for ozone generation and air pollution control, Ind. Eng. Chem. Res. 47 (2008) 2122–2130.
[8] T. Yamamoto, K. Pamanathan, P.A. Lawless, D.S. Ensor, J.R. Newsome, N. Plaks, G.H. Ramsey, Control of volatile organic compounds by an ac energized ferroelectric pellet reactor and a pulsed corona reactor, IEEE Trans. Ind. Appl. 28 (1992) 528–534.
[9] S. Futamura, A.H. Zhang, T. Yamamoto, The dependence of nonthermal plasma behavior of VOCs on their chemical structures, J. Electrostat. 42 (1997) 51–62.
[10] S. Futamura, A.H. Zhang, H. Einaga, H. Kabashima, Involvement of catalyst materials in nonthermal plasma chemical processing of hazardous air pollutants, Catal. Today 72 (2002) 259–265.
[11] S. Futamura, A.H. Zhang, T. Yamamoto, Mechanisms for formation of inorganic byproducts in plasma chemical processing of hazardous air pollutants, IEEE Trans. Ind. Appl. 35 (1999) 760–766.
[12] J.S. Chang, P.A. Lawless, T. Yamamoto, Corona discharge processes, IEEE Trans. Plasma Sci. 19 (1991) 1152–1166.
[13] K. Takaki, K. Urashima, J.S. Chang, Ferro-electric pellet shape effect on C_2F_6 removal by a packed-bed-type nonthermal plasma reactor, IEEE Trans. Plasma Sci. 32 (2004) 2175–2183.
[14] B. Eliasson, U. Kogelschatz, Nonequilibrium volume plasma chemical processing, IEEE Trans. Plasma Sci. 19 (1991) 1063–1077.
[15] T. Oda, Y. Yamashita, K. Takezawa, R. Ono, Oxygen atom behaviour in the nonthermal plasma, Thin Solid Films 506/507 (2005) 669–673.
[16] M. Magureanu, N.B. Mandache, P. Eloy, E.M. Gaigneaux, V.I. Parvulescu, Plasma-assisted catalysis for volatile organic compounds abatement, Appl. Catal. B: Environ. 61 (2005) 12–20.